

DESIGN, CONSTRUCTION AND TESTING OF A TURBOMOLECULAR PUMP WITH FIVE AXES MAGNETIC SUSPENSION

Luigi Mazzocchetti, Enrico Rava

Elettrorava S.p.A., Savonera, Torino, Italia

Cristiana Delprete, Giancarlo Genta

Dipartimento di Meccanica, Politecnico di Torino, Torino, Italia

Stefano Carabelli

Dipartimento di Automatica ed Informatica, Politecnico di Torino, Torino, Italia

ABSTRACT

A turbomolecular pump with five-axes magnetic suspension has been designed and built in 1993 as a result of a co-operation between the Elettrovava S.p.A. and the Laboratory for Mechatronics of Politecnico di Torino. The design and the construction of the pump are here described, together with some problems which have been encountered and solved during the construction stage. A dynamic analysis of the closed-loop system has been performed before the construction to make sure that the system stability was achieved over the entire operational range. Two prototypes with a total rotor mass of about 10 kg running at 27000 rpm have been built and tested, and some minor modifications are now in process in order to start series-manufacturing. The tests on the prototypes have given very satisfactory results: vibration and power consumption are very low compared with a conventional turbomolecular pump with ball bearings, and the agreement between theoretical predictions and actual behaviour is very good.

INTRODUCTION

The advantages of a magnetic suspension for high speed rotating machinery and particularly for turbomolecular pumps are now well established. Turbomolecular pumps operating on conventional ball bearings are now considered inadequate for some applications, mainly owing to the contamination of vacuum due to vapours of the bearing lubricant. Turbomolecular pumps with magnetic bearings can be built following a number of different layouts, spanning from a hybrid configuration with a conventional rolling element bearing on the "motor side" and a passive, permanent magnet bearing on the "high-vacuum side"

to a full five-active-axes solution. The choice between them is a complex trade-off, in which considerations on performance, cost and available technology play an important role. Generally speaking, solutions based on passive bearings, with only one active axis or even a conventional bearing taking care of the stability, seem more adequate for small machines while solutions based on a complete active suspensions can be considered with advantage for larger sizes.

After having built a prototype of a small hybrid machine [1], [2] and started to produce a line of small pumps of that type, the possibility of building a prototype of a machine with a five active axes suspension was investigated by Elettrovava. In the meantime, a spindle based on the same technology was built and tested by the authors [3]. The very good performance of the prototype allowed to be confident on the success of the project.

Among the complete line of turbomolecular pumps with conventional ball bearings already manufactured by Elettrovava since many years, the model with a pumping speed of 1800 l/s has been chosen. The 1800 l/s turbopump is well suited for vacuum systems used in semiconductor production, where the low vacuum contamination requirement is of the utmost importance, and its size is large enough to fall in the field where a fully active suspension seems to be more suitable, as the cost of the electronic controller is moderate, compared with that of the electro-mechanical parts of the machine. However, magnetic suspensions for 500 and 1000 l/s turbopumps are in project.

The aim of the paper is to describe the work performed on the prototypes of the machine, including the design and construction of the pump and the controller, the structural and dynamic analysis and the first experimental test results.

DESIGN AND CONSTRUCTION OF THE PUMP

The basic layout of the conventional machines built by Elettrorava is maintained with the minimum of adjustments required by the introduction of the new technology, as consistent with the cost and time constraints imposed to the whole project. Larger design changes, necessary to optimise the project and to obtain the maximum advantages from active magnetic suspensions, were planned for a subsequent development stage after having solved the basic problems directly linked with the bearing system.

A schematic cross section of the first prototype of the ETP 1800-M turbopump with five axes magnetic suspension is shown in figure 1. The pumping section of the rotor is composed by eleven bladed discs which are mounted on the shaft by heat shrinking. The discs are made of a light alloy (2024 UNI 3583) while the shaft is made of a ferromagnetic steel. The first and the last rotor discs are provided with a balancing device patented in the past by Elettrorava and now common in all its production units. It is based on a disc in which some screws can be moved within threaded holes to perform the dynamic balancing of the rotor. The lower section of the unit houses the three-phases asynchronous a.c. induction motor with copper squirrel cage rotor. As the operating speed of the machine is 27000 rpm, the two poles motor works at a nominal frequency of 450 Hz.

The two magnetic actuators of the radial bearings are located at the sides of the motor. The general layout of the actuators is similar to that of an induction motor, the only difference being in the number and the type of the coils. A detailed description of the actuators is reported in [3].

While in the spindle described in [3] the sensors were commercial inductive probes, in the present case also the sensors were designed and purposely built for the application. They are differential inductive sensors driven at high frequency which ensure a very good linearity and thermal stability. The general layout is very similar to that of the actuators, the only difference being in the lower axial length and smaller section of the conductors.

The choice of building the sensors for the application proved to be very successful, both from the technical and economical viewpoint, and allowed to reduce the time delay between the completion of the prototype and the starting of the design of a production machine. All the rotors of the motor, actuators and sensors are laminated to minimise the eddy current losses. The radial bearings stators are made in low loss factor iron sheets with eight equal slots. A picture of the stators and the shaft with the laminated rotors assembled on it is shown in figure 2. The copper windings are connected in such a way to get a SNNSSNNS magnetic

field configuration. This choice has been done in order to minimise the eddy current losses in the rotors (figure 3). The upper radial bearing has been located as near as possible to the centre of gravity of the rotor, and it is larger than the lower one to support the overhang weight of the rotor in horizontal position. The axial thrust disc is mounted at the lower edge of the shaft and between the two axial electromagnets, in front of the axial inductive position sensor. The axial sensor is a differential sensor similar, in principle, to the radial ones. It operates measuring the distances with respect to two surfaces, one being the lower end of the shaft and the other the upper surface of a threaded element which can be moved axially to mechanically change the reference level. The emergency bearings are located at the ends of the shaft and they are dry lubricated ceramic ball bearings. Their location allows a quick maintenance when they must be replaced without the need of disassembling the high vacuum bladed stator. An optical detector is focused on the rotor to supply a signal for monitoring the rotational speed and for triggering the automatic balancing electronic circuit. The body of the pump is made of aluminium alloy and the high vacuum envelope is made of AISI 304 stainless steel.

During the construction of the prototype, the design of the pump was modified in order to improve the performances and solve some problems which have been encountered. The main characteristics of the pump are summarised in table 1. The aspects that had to be analysed and taken into account are:

- the location of the position sensors to have a satisfactory observability of rigid and bending modes;
- the electromagnetical interference between sensors and actuators that can play an important role when using switching amplifiers. The sensors have to be shielded and their geometrical dimensions must be minimised;
- the roundness and homogeneity errors of the laminated rotors of the sensors. These errors have to be minimised to achieve a satisfactory operation.

DESCRIPTION OF THE CONTROLLER

The controller contains the following circuits:

- position sensors oscillator, sensors signal conditioning circuits and five control networks for radial and axial bearings;
- power supplies, three phases inverter and power conditioner for the motor, kinetic energy recovery circuit and microprocessor based control and monitoring card.

The position sensor coils are connected in a Wheatstone bridge and are driven by a 40 kHz oscillator.

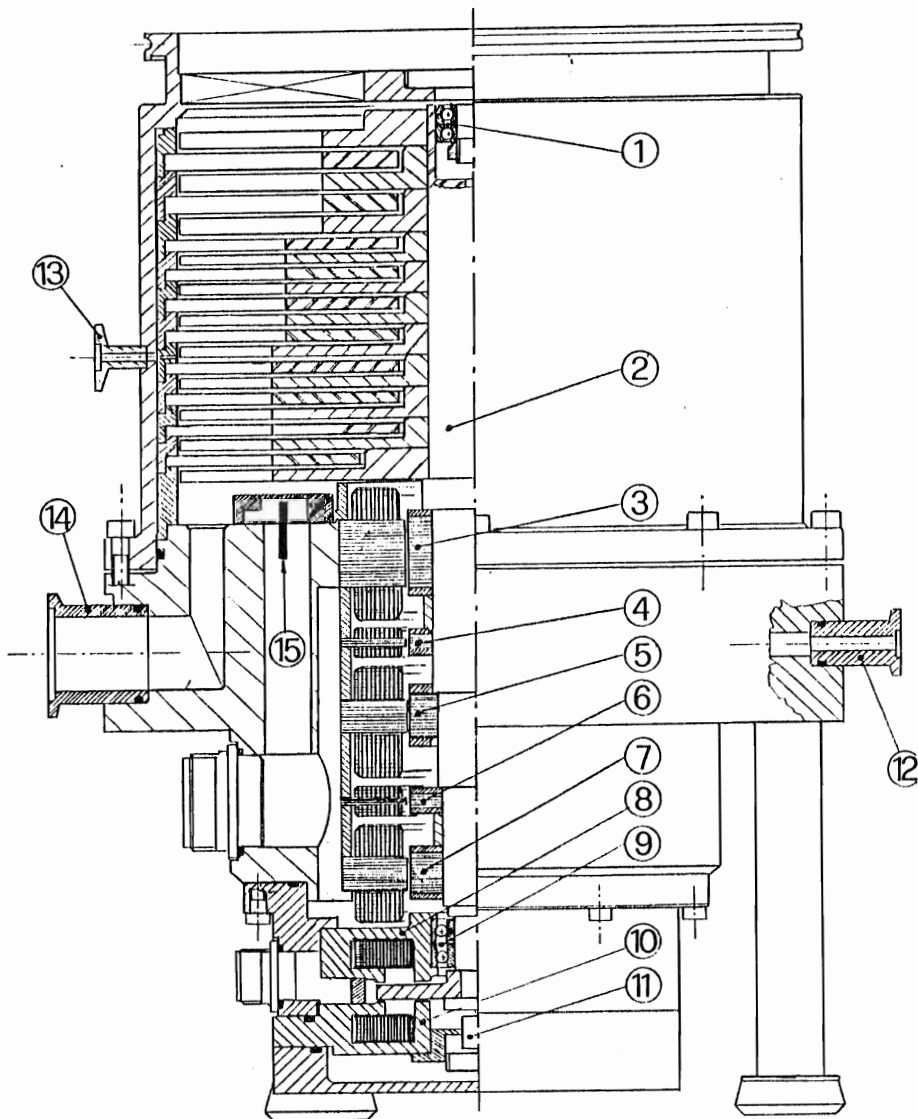


FIGURE 1: Sketch of the machine. 1, 9 emergency bearings; 2 shaft; 3, 7 radial actuators; 4, 6 radial sensors; 5 electric motor; 8, 10 axial actuator; 11 axial sensor; 12 inert gas inlet; 13 venting flange; 14 forevacuum connection; 15 speed sensor.

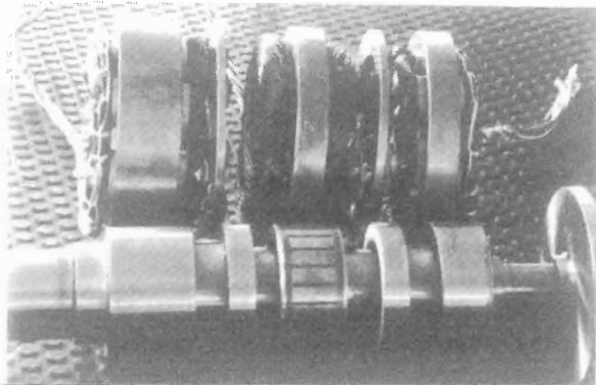


FIGURE 2: Stators of the radial actuators, sensors and of the electric motor together with the shaft.

The signal from the bridge is amplified by a floating input differential amplifier and demodulated by means of a synchronous rectifier circuit and filtered by a low-pass filter. The magnetic bearing controller is a PI plus lead-lag compensating network which has a 10 dB/dec gain slope characteristic and a constant 40° phase lead over the entire operating frequency range. The MOSFET transistor switching amplifiers work at 48 kHz and have a very high efficiency. With an adequate choice of the circuit parameters the frequency bandwidth of such current amplifiers is about 5 kHz.

A special tracking feed-forward filter cancels the synchronous component from the radial sensors signal. Therefore the rotor is allowed to rotate about its

principal axis of inertia and the vibration level on the body of the pump is very low (automatic balancing).

In case of power failure, the kinetic energy of the rotor is used to supply the power needed for the magnetic suspension. A special circuit performs a controlled deceleration ramp and the induction motor acts as a generator from 27000 rpm to 6000 rpm when a safe landing occurs on the emergency bearing.

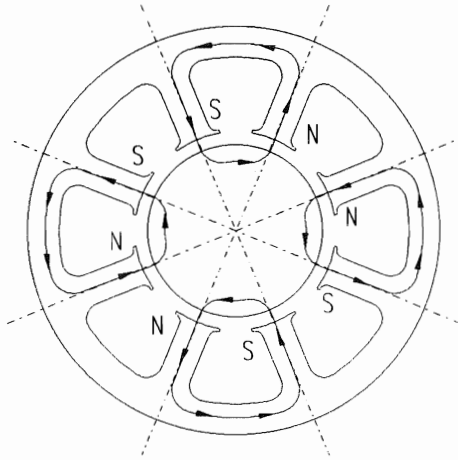


FIGURE 3: Polarity of the actuator coils.

TABLE 1: Characteristics of the pump.

Pumping speed for nitrogen	1800	l/s
Rotor mass	10	kg
Rotational speed	27000	rpm
Rotor diameter	260	mm
Peripheral speed	367	m/s
Upper bearing maximum radial load	300	N
Lower bearing maximum radial load	150	N
Maximum thrust load	600	N
Maximum motor power	500	W
Total power consumption (including electronic control) at limit vacuum	50	W
Starting time	600	s
Operating position	any	

DYNAMIC AND STABILITY ANALYSIS

The dynamic analysis was performed using the DYNROT 4.1 finite element rotordynamics code [4]. A FEM model was built using 30 Timoshenko beam elements to model the shaft, 16 mass elements for the rotors of the actuators, sensors, motor and for the various bladed discs and two magnetic bearing elements.

A sketch of the model is shown in figure 4a. The total number of the complex degrees of freedom involved in the flexural analysis was 62, later reduced to 31 through Guyan reduction by considering as slave degrees of freedom all rotations at the nodes.

The moment of inertia of the rotor computed by the code ($2.92 \cdot 10^{-2} \text{ kg m}^2$) is very close to the measured value ($2.94 \cdot 10^{-2} \text{ kg m}^2$). The stator of the machine was modelled as a rigid body and no damping of the structural parts was considered in the analysis.

A first analysis was aimed to the computation of the critical speeds and mode shapes of the uncontrolled rotor. The first four mode shapes are shown in figure 4b. The critical speeds corresponding to the two rigid body modes are obviously equal to zero, while the two following critical speeds are at 5410 rad/s (51660 rpm) and 13922 rad/s (132950 rpm). Both are well above the maximum operating speed: the machine operates in the whole working range well below the critical speeds linked with deformation modes of the shaft.

The Campbell diagram of the uncontrolled system was also plotted, obtaining that the natural frequencies related to the deformation modes of the rotor are strongly influenced by the spin speed: the first deformation mode occurring at 3630 rad/s (578 Hz) at standstill, 4465 rad/s (711 Hz) at the operating speed and 5410 rad/s (861 Hz) in synchronous whirling (first deformation critical speed).

The mode shapes are also influenced by the speed: those corresponding to the first bending mode are shown in figure 4c. The corresponding values for the second mode are respectively 7885 rad/s (1255 Hz), 8933 rad/s (1422 Hz) and 13922 rad/s (2216 Hz).

TABLE 2: Controlled system's critical speeds

Critical speed rad/s (rpm)	Decay rate 1/s	Note
256 (2445)	88	Rigid body mode
1425 (13610)	588	Rigid body mode
5225 (49895)	28000	Controller mode
5717 (54590)	-6	Deformation mode

TABLE 3: System's natural frequencies at standstill

Natural freq. rad/s (Hz)	Decay rate 1/s	Note
234 (37)	88	Rigid body mode
1293 (206)	502	Rigid body mode
3755 (598)	37	Deformation mode
5246 (835)	50095	Controller mode

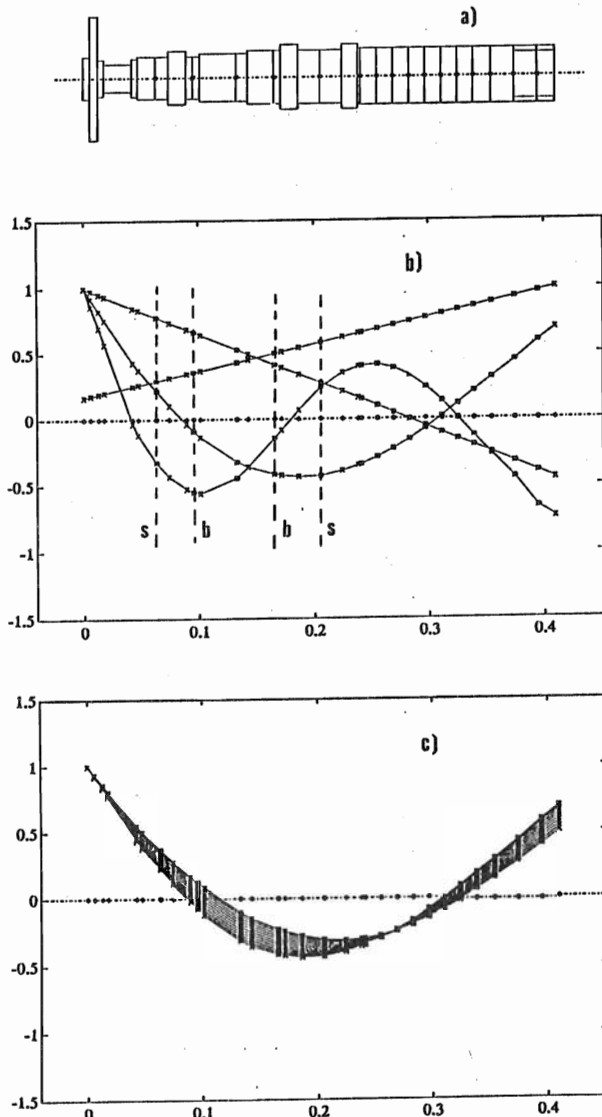


FIGURE 4: a) rotor's FEM model; b) mode shapes at the first four critical speeds of the uncontrolled system. (s: sensors, b: bearings); c) mode shapes of the first flexible forward mode at various speeds

The dynamic analysis of the controlled system was then performed. DYNROT code allows to model the controller of magnetic bearings as a PID controller or as a general controller, assigning directly its transfer function [4]. Assuming the following transfer function

$$C(s) = 7.5 \frac{0.5s + 1}{0.5s} \frac{2 \cdot 10^{-2}s + 1}{5 \cdot 10^{-3}s + 1} \frac{8 \cdot 10^{-4}s + 1}{2 \cdot 10^{-4}s + 1} \frac{1}{3.2 \cdot 10^{-5}s + 1}$$

the values of the first four critical speeds and corresponding decay rates shown in table 2 were obtained. The critical speed corresponding to the first

deformation mode has a negative decay rate and causes instability. This however does not cause any inconvenience, as no operation in the supercritical field with respect to deformation modes was planned.

The values of the first four natural frequencies at standstill are reported in table 3. It is clear that all the modes considered are stable; similar results were obtained for the whole working range by plotting the Campbell diagram and the plot of the decay rate versus the spin speed.

The only issue which could raise some doubts is the high value of the second rigid body critical speed. Actually, both rigid body critical speeds are very well damped, particularly the second one. The decay rate at the second one is so high that it is easily predictable that its crossing will be barely detectable.

TESTS AND EXPERIMENTAL RESULTS

Many tests have been performed on the pump and the controller in order to verify the theoretical predictions:

- rigid body and bending modes frequencies at standstill with spectrum analyser;
- power consumption in different operating conditions;
- kinetic energy recovery;
- evaluation of the total drag losses;
- horizontal and vertical operating position tests;
- dynamic balancing at 9000 rpm with "EQUIL" code;
- automatic balancing test;
- vibration measurements during operation.

Vibration tests were performed using impulsive excitation and measuring the response with accelerometers and HP Dynamic Analyser 35660A. The most important rigid body mode was measured at a frequency of 90 Hz. This frequency lays between the two computed values, which however are not directly comparable with the experimental result: the high value of the decay rate makes the peak of the response curve to be located at a frequency not coincident with the poles of the system. The first two bending modes of the rotor occur at 624 Hz and 1350 Hz, close enough to the computed values of 598 and 1255 Hz.

The power dissipated in all switching amplifiers and electromagnets is 13 W when the pump is in vertical position. The power absorbed by the motor is 35 W when the pump is running at 27000 rpm under high vacuum. These losses can be ascribed to the electric motor, to magnetic bearing rotor losses and gasdynamic drag. The total power is then 48 W, so low that the pump does not need to be cooled when running at high vacuum. The machine compares very favourably with similar machines of the same size running on conventional bearings: a normal figure for the power is of about 250 W.

The kinetic energy recovery circuit has been tested with good success. At the beginning of the deceleration ramp it can provide more than 200 W, that is much more than needed. When the rotational speed approaches 6000 rpm, the supplied power is very close to 13 W, which is just the power needed for the magnetic suspension. At lower speed the rotor lands on the emergency bearings, unless a battery is used to keep the magnetic suspension working.

The total drag on the rotor (due to the bearings, the motor and gasdynamic causes) has been evaluated by plotting a spin-down curve and evaluating the deceleration rate. From the measured value of the moment of inertia of the rotating system a total power loss of 35 W was computed; 25 W can be ascribed to the motor and 10 W to the magnetic bearings and to the gasdynamic drag at a pressure of 0.05 mbar.

The pump was tested in three different positions: vertical, vertical upside-down and horizontal. Some minor modifications had to be done on the controller to get a satisfactory operation in any position. In horizontal position the power dissipated in the magnetic bearings was of course higher due to the strong magnetic field in the radial bearings needed to sustain the weight of the rotor.

The dynamic balancing of the rotor was performed at low speed in just three runs, using the signals from the radial sensors to detect the unbalance. This balancing procedure was aimed to reduce most of the rotor unbalance and not to achieve a balancing grade as accurate as needed on conventional machines.

The automatic balancing circuit allows then to obtain very low vibration levels at high speed, mainly due to deformation of the rotor. The vibration level measured by an accelerometer on the pump body at the working frequency of 450 Hz was really very low: 0.006 μm .

CONCLUSIONS

The main features of a turbomolecular pump based on active magnetic bearing technology have been described. The two prototypes built were subjected to a number of tests and proved to work in a very satisfactory way to the point that the first production units are now being designed.

The predictable advantages of very low vacuum contamination, low drag torque and very smooth running without the need of very strict balancing tolerances which are usually associated with magnetic bearings have been fully achieved. As an additional feature, the magnetic suspension has a very low power consumption. This was achieved by resorting to switching amplifiers which require just about 13 W to maintain the 10 kg rotor in levitation with the machine in vertical position.

The kinetic energy recovery circuit proved to be effective in maintaining the rotor in its levitated position during the spin-down following a power failure. The rotor lands on the emergency bearings at a speed of about 6000 rpm, low enough to prevent damages to the rotor and the emergency device. A solution in which the emergency ball bearings are substituted by simple bushes is under study and will be considered for the production machine.

One of the most critical aspects determining the possible acceptance on the market of machines based on magnetic bearings is the overall cost. While a definite assessment on the cost of the machine cannot be based on an experimental prototype as the one here presented, particular attention was devoted to economical features in the whole project. The design of the actuators and sensors is very promising from this viewpoint.

At present the first production machine is being designed: it will include many refinements, aimed to reduce the overall size and the mass of the rotating parts and to keep production costs as low as possible.

REFERENCES

- [1] Genta G., Mazzocchetti L. and Rava E., Magnetic Suspension for a Turbomolecular Pump, Proc. of the 2nd Int. Symp. on Magnetic Bearings, Japan, 1990.
- [2] Genta G., Delprete C., Tonoli A., Rava E. and Mazzocchetti L., Study of the Geometry of a Radial Passive Magnetic Bearing for Application to a Turbomolecular Pump, Proc. of the 3rd Int. Symp. on Magnetic Bearings, Virginia, 1992.
- [3] Delprete C., Genta G. and Carabelli S., Design, Construction and Testing of a Five Active-Axes Magnetic Bearing System, Proc. of the 2nd Int. Symp. on Magnetic Suspension Technology, Washington, 1993.
- [4] Genta G., Carabelli S. and Delprete C., Active Magnetic Bearing Control Loop Modelling for a Finite Element Rotordynamics Code, Proc. of the 2nd Int. Symp. on Magnetic Suspension Technology, Washington, 1993.